International Journal of Multimedia and Ubiquitous Engineering
Vol.10, No.4 (2015), pp.1-10
http://dx.doi.org/10.14257/ijmue.2015.10.4.01

The Research on Algorithm of Flame Field Fast Compression

Zhenhua Wei and Xiaoyuan Yan

(North China Electric Power University, School of Control and Computer Engineering, No.2,Road Beinong, Huilongguan Town, Changping District, Beijing, China,102206)
474029557@qq.com

Abstract

3D graphics technology is one of the important research direction in the field of graphics currently. 3D graphics technology has very broad application prospects, and it has very important application value in the field of scientific research, military, education, industry, medical, entertainment and many other fields. But the data volume of high resolution 3D graphics is huge, and the storage, transmission and real-time display higher requirements are put forward. In recent years, people have shown strong interest in the research of 3D graphics compression techniques. In this article, the 3D graphics compression technology and the combination of industrial flame are be combined to introduces a compression method for three-dimensional flame.

Keywords: *Flame field, Characteristics of Topology, Matching Feature Points, Delaunay Triangulation*

1. Introduction

With the development of information technology, 3D graphics are widely used in multimedia communications and computer systems, but the large amount of information is a striking feature of image data. If a huge amount of data without compression, is not only beyond the computer storage and handling ability, and under the existing communication channel transmission rate is unable to complete a large number of multimedia real-time transmission. Therefore, in order to more effective storage, processing and transmission of the image data, must be compressed. In recent years, much attention has been paid to 3D graphics compression technology appear some of the more mature theory and algorithms. The purpose of this article is combine the 3D graphics compression technology with the combination of industrial flame and provide a algorithm of quickly compress storage 3D flame, based on the research of 3D graphics compression technology.

2. Edge Detection

The commonly used edge detection [1] is divided into two types. One is an edge detection operator based on first derivative, it detect image edge by calculating image gradient values, such as: Roberts operator, Sobel operator, Prewitt operator; The other is an edge detection operator based on second derivative, it detect image edge by seeking the second derivative of the zero point, such as: the Laplacian operator, LOG operator, Canny operator. In this article, Canny [2-3] operator is applied for the edge detection of 3D flame graphs.

In 1986, Canny put forward a good operator shall meet the following criteria:

(1) SNR criterion, that is, don't miss detect real edge, and did not take the non-edge points as the edge point check out, make the output of signal-to-noise ratio maximum.

ISSN: 1975-0080 IJMUE

(2) Positioning accuracy criterion, that is, to detect the edge points in the center of the actual edge as much as possible.
(3) Single edge response criterion, that is, the probability of single edge effects multiple response should be lower, the false edge response should get maximum limit.

It can get optimal detection operator by combine the three criterion of Canny, so the Canny operator has a good performance of edge detection. The algorithm is by looking for local maximum values of the image gradient, the first-order differential of Gaussian function can be used to calculate the gradient. In the arithmetic, it detect strong and weak edge by two thresholds respectively, if and only if the weak edge connect to the strong edge, the weak edge will be output. So, the Canny algorithm is not susceptible to noise interference, it can get favorable equilibrium in noise and edge detection and detect the real weak edge.

Canny operator of the specific steps is as follows:

Firstly, using two-dimensional Gaussian filter template for filter to eliminate noise. The σ is a parameter of the Gaussian filter, it controls the degree of smooth.

$$G(x,y)=\frac{1}{2\pi\sigma^2}\exp\left(-\frac{x^2+y^2}{2\sigma^2}\right) \quad (1)$$

Secondly, using derivative operator (Prewitt operator, Sobel operator, for example) to find the derivative of (Gx,Gy) image gray level along the two directions, and calculate the size of the gradient and the gradient direction.

$$|G|=\sqrt{G_x^2+G_y^2} \quad (2)$$

$$\theta = Arc\tan\left(\frac{G_x}{G_y}\right) \quad (3)$$

The edge of the gradient direction roughly divided into four types(horizontal, vertical, direction, 45 degrees and 135 degrees type). Comparing with different neighboring pixels in all directions, to determine the local maximum values. If a pixel gray value is small than the gray value of gradient direction before and after the two pixel, then set the pixel values to 0, that is not the edge, this process is called "the great curb".

The cumulative histogram is used to calculate the two thresholds, which is greater than the high threshold must be edge, and which is less than the low threshold must not be edge. If the test result is greater than the low threshold, but less than high threshold, it depends on if the pixels in the adjacent pixels greater than high threshold of edge pixels, if so then it is edge, otherwise it is not the edge.

Using Canny operator for edge detection results are shown in Figure 1.

Figure 1. Edge Detection

3. Topological Feature Extraction

There could use two steps followed to abstract the whole closed contour[4]. First, the canny operator was taken to abstract boundaries in different scale. The boundary was constituted by the grayscale radical changed parts. In differential geometry, the gradient direction is the most dramatic changes in direction. Hence, The maximum value along the gradient direction of gray level changed corresponds to the boundary, which is,

$$\begin{cases} \partial^2 R(x,y,\sigma)/\partial v^2 = 0 \\ \partial^3 R(x,y,\sigma)/\partial v^3 < 0 \end{cases} \tag{4}$$

In expression (4), the direction angle of the gradient direction (v) is shown in $\varphi=\arctan(Ry/Rx)$, and the directional derivative operator could be express as $\partial R/\partial v=\{\partial R/\partial x,\partial R/\partial y\}\cdot\{\cos\varphi,\sin\varphi\}$。The figure of using canny operator under different scales boundary extracted is figure 2. It shows that the main boundary could be obtained in the coarser scales when the thresholds is larger, however, these discontinuous boundaries could not reflect the complete target contour. More details description of the boundary could be got on a finer scales when the thresholds is smaller, nevertheless, it would contain more pseudo boundary caused by noise.

Figure 2. Characteristics of Topology

Then, based on the multi-scale Canny operator to extract the boundary of evolution law of track them in different scales, and according to the boundary of the importance of sorting, keep the important boundary, abandon the boundary of the secondary, fully closed image contour map.

$$S_i = \sum_{\sigma=\sigma e}^{\sigma d} \frac{F_i(\sigma) - \overline{F(\sigma)}}{\mathrm{var}(F(\sigma))} \tag{5}$$

$$\overline{F(\sigma)} = \frac{1}{M}\sum_{i=1}^{M} F_i(\sigma) \tag{6}$$

$$\mathrm{var}(F(\sigma)) = \sqrt{\frac{1}{M}\sum_{i=1}^{M}\left(F_i(\sigma) - \overline{F(\sigma)}\right)^2} \tag{7}$$

The importance of boundary is decided by its stability and amplitude. Amplitude show that edge luminance change intensity, and stability refers to the edge of the life cycle. Type (5), (6) and (7), Si expressed as the importance of the edge i. To take $F_i(\sigma)$ as the edge of the scale of the Canny operator. M for the total number of edges scales σ. $\overline{F(\sigma)}$ and var(F(σ)) are on behalf of all scales on the edge of the mean and variance. Measuring stability by the boundary of life cycle. Article number of the space on the adjacent boundary under large scale could be merged into one, some boundaries in large scales could disappear in a finer scales. Σe and σd said the scale of the edges appear and disappear, respectively. Therefore, the larger the boundary length, and the background contrast the intense, life cycle, the longer the border the higher its important degree. The importance of this definition may be negative, in order to avoid appear this kind of situation, was revised:

$$S_i^{rec} = \begin{cases} S_i + 1 & S_i \geq 0 \\ e^{S_i} & S_i < 0 \end{cases} \tag{8}$$

The edge of the revised importance Approximation to the mean is 1, the distribution of the variance of 1.

4. Selecting and Matching Feature Points

4.1. Feature Point Extraction Method

Commonly used feature point extraction methods include Wavelet Transform, corner extraction method and interest operator method [5].

In order to strike the feature points of the image, we use a simple method proposed by Moravec for obtaining an image feature points. Moravec [6] defines image feature points as interest points, which have a larger variance rate of gray level in all directions. Moravec operator to strike interest points is defined as interest operator. The operator is used to strike the variance rate of gray level of each image in the horizontal, vertical and two diagonal directions. The minimum value of gray level change rate in each direction is assigned to be the gray level change rate of the pixel .

Within a range of 5×5 In this point as the center

Set the current point as the center. Within a range of 5×5, the specific formula of the variance rate of gray level in all directions is as follows:

Gradation change rate in the horizontal direction:

$$V_1 = \sum_{x=0}^{4}\sum_{y=0}^{3}\left[g(x,y) - g(x,y+1)\right]^2 \tag{9}$$

Gradation change rate in the vertical direction:

$$V_2 = \sum_{x=0}^{3}\sum_{y=0}^{3}\left[g(x,y) - g(x+1,y)\right]^2 \tag{10}$$

Gradation change rate of 135 degrees in the diagonal direction:

$$V_3 = \sum_{x=0}^{3}\sum_{y=0}^{3}\left[g(x,y) - g(x+1,y+1)\right]^2 \tag{11}$$

Gradation change rate of 45 degrees in the diagonal direction:

$$V_4 = \sum_{x=0}^{3}\sum_{y=0}^{4}\left[g(x,y) - g(x+1,y-1)\right]^2 \tag{12}$$

Where g(x,y) denoted as g_{xy} is the gradation value of the pixel (x,y). Mar is Moravec output values of the pixel:

$$Mar = \min\{V_1, V_2, V_3, V_4\} \tag{13}$$

Typically in the area where gray level change rate is bigger, a large number of interest points will appear as groups. In the smooth gray area, there are few interest points. In order to better extract important interest points to reflect the image feature, we use adaptive threshold feature point extraction methods.

First, distinguish the feature area and the non-feature area according to the value of the pixel Mar. Take M×N blocks and calculate Mar_{sum}.

$$Mar_{sum} = m\sum_{x=0}^{M}\sum_{y=0}^{N} Mar(x,y) \tag{14}$$

Set a threshold value and divide the image into feature area and non-feature area. If Mar_{sum} is greater than the threshold, the block is set to the feature block. If not, the non-feature areas. That is:

$$\begin{aligned} Mar_{sum} > threshold &\rightarrow \text{特征区} \\ Mar_{sum} \le threshold &\rightarrow \text{非特征区} \end{aligned} \tag{15}$$

For the feature region, taking into account the relatively rich image detail, more feature points will be extracted. For the non-feature region, less feature points will be extracted.

4.2. Feature Point Extraction Results

Figure 3 is a perspective view of the image on the left. Figure 4 is the result of the left view after extracting feature points with Moravec method and the white points are the feature points. Where the size of the feature area is 6×6 pixels square and that of non-feature areas is 12×12 pixels square.

Figure 3. The Original View

Figure 4. Feature Points Distribution

4.3. Images Matching

Assuming $I_1(x,y)$ is the imaging of the region and $I_2(x,y)$ contains not only the region but also other regions which are connected the region. Then the image matching is the mapping of spatial location and gray between the two images. That is:

$$I_2(x, y) = I_1(f(x, y)) \tag{16}$$

Where f is two-dimensional spatial coordinate transformation. It becomes (x,y) to (x',y') and that means (x',y')=f(x,y).Matching problem is to find the optimal spatial transformation f to achieve purposes of localization and identification. The model f can be expressed as:

$$\begin{pmatrix} x' \\ y' \end{pmatrix} = R \begin{pmatrix} \cos\theta & \sin\theta \\ -\sin\theta & \cos\theta \end{pmatrix} \begin{pmatrix} x \\ y \end{pmatrix} + \begin{pmatrix} c \\ d \end{pmatrix} \tag{17}$$

Where R is a scale factor, θ is the rotation angle of the two-dimensional plane and c and d are the displacement factors of the two-dimensional plane. Image matching is actually optimal estimation of these parameters.

In this paper, normalized co-variance matching method [7] is used to match the feature points of stereogram. First, take a feature point P1(i,j) from the left view where feature points have been extracted, then take (i,j) as center in the right view and take a M×N rectangle. Measure the similarity between P1 and each point Pi in the rectangle. The point with maximum similarity is the matching point. Match each point of the left view and the right view orderly and finally obtain all the matching feature point pairs.

Similarity measurement of Pi and P1 is represented by the normalized covariance correlation value of sub-regions in the relevant image window (2k+1)(2l+1).

Take the feature point of left view P1(i,j) and the feature point of right view $P_2(i,j)$. Set gray values of (i,j) in the left and right view as $I_1(i,j)$ and $I_2(i,j)$. Normalized covariance can be defined as:

$$c(P_1, P_2) = \frac{\operatorname{cov}(i, j)}{\sqrt{\operatorname{var}(i, j, I_1)\operatorname{var}(i, j, I_2)}} \tag{18}$$

Window size:

$$M = (2k+1)(2l+1) \tag{19}$$

Where 2k+1 and 2l+1 are the length and width of the window.

The selected window gray covariance of the left and right view:

$$\operatorname{cov}(i, j) = \frac{1}{M}\sum_{m=-k}^{k}\sum_{n=-l}^{l}\left[I_1(i+m, j+n) - \overline{I_1(i, j)}\right] \times \left[I_2(i+m, j+n) - \overline{I_2(i, j)}\right] \tag{20}$$

Gray variance within the selected window of left view:

$$\operatorname{var}(i, j, I_1) = \frac{1}{M}\sum_{m=-k}^{k}\sum_{n=-l}^{l}\left[I_1(i+m, j+n) - \overline{I_1(i, j)}\right]^2 \tag{21}$$

Gray variance within the selected window of right view:

$$\operatorname{var}(i, j, I_2) = \frac{1}{M}\sum_{m=-k}^{k}\sum_{n=-l}^{l}\left[I_2(i+m, j+k) - \overline{I_2(i, j)}\right]^2 \tag{22}$$

—I1(i,j)and —I2(i,j) are average gray within the selected windows of left and right views:

$$\overline{I_1(i, j)} = \frac{1}{M}\sum_{m=-k}^{k}\sum_{n=-l}^{l} I_1(i+m, j+n) \tag{23}$$

$$\overline{I_2(i, j)} = \frac{1}{M}\sum_{m=-k}^{k}\sum_{n=-l}^{l} I_2(i+m, j+n) \tag{24}$$

4.4 Image Matching Results

With normalized covariance method match the Figure 4 and Figure 5 in section 4.1 one by one . So obtain the matching feature points in the right view.

Figure 5. Results of Image Matching

5. Partitioning

Given point set $\{P_i\}$,i=1......N, existing polyhedron $\{V_j\}$,j=1......N, and the matching, including each polyhedron $\{V_j\}$contains and only contains a point P_i, V_j to each point P_i in the distance is less than that point $\{P_i\}$ to the outside P_i in addition to any other point in the distance, namely

$$V_i = \{P : \left|P - P_j\right| < \left|P - P_i\right|, \forall i \neq j\} \tag{25}$$

Delaunay triangulation is Voronoi diagram [8] of the accompanying figure, it is the Russian mathematician Delaunay is put forward in 1934, he points out: for planar domain

N scattered point set, exists and there is only one kind of triangle subdivision, made all the sum of the minimum Angle of the triangle to the maximum, generally called Delaunay triangle subdivision.

According to the implementation process, the various algorithms of generating Delaunay triangulation net is divided into three categories: partition algorithm, point by point insertion method and triangulation method of growth. This article USES the triangle net growth in the triangle subdivision of the image.

Green and Sibson realized the growth of a Dirichlet generated polygon graph algorithm for the first time [9]. Brassel and Reif also made similar algorithm. McCullagh and Ross block and sorting through the collection of improved search methods, to reduce the search time. Maus also shows a very similar algorithm.

Triangular mesh generation algorithm is the basic steps:

(1) as a starting point.

(2) to find out and starting point for the recent data points are connected to form a Delaunay triangle as a baseline, according to two basic properties of Delaunay, find the third point and the baseline Delaunay triangle.

(3) the baseline two endpoints linked to the third point, become the new baseline.

The above two steps (4) iteration until all baseline is processed.

This process, the results showed that the growth of triangulation algorithm idea is, to find out some concentrated shortest distance between two connected as a Delaunay edge, and then according to the nature of the Delaunay triangulation net to find containing the Delaunay triangle on the side of another endpoint, in order to handle all the new generation side, until the final.

This chapter to get the extracted feature points in the previous chapter left view figure 4-2 Delaunay triangle subdivision. At an Angle of feature points and four point for point set subdivision, and defines the image edge of the up and down or so for the edges in the triangulation. Decomposition of profile control as shown in Figure 6.

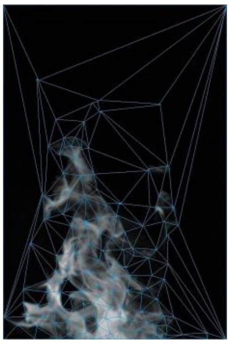

Figure 6. Result of Partitioning

6. Morphing

Image deformation [10] based on Delaunay triangle subdivision method, on the whole, similar to the method based on grid deformation. First given two images, respectively called I_s and I_d, immediately source image and target image, then defined a series of corresponding control point pairs in the two images, by the control points on the source image series and four vertices on source image rectangular area, can construct a Delaunay triangulation on the source image. All the triangles in the Delaunay triangulation formed a source controlling grid M_s, its shape jointly confirmed by the coordinates of control points and Delaunay triangulation algorithm. The second grid M_d specifies the corresponding position in the target image.

Because the triangle mesh Ms and Md is limited to topological isomorphism, the triangles in the grid are one-to-one correspondence, and they a complete coverage of I_s

and I_d of the corresponding image formation, so the whole image of the deformation can be reduced to deformation of the corresponding triangular area.

Assumption, there are two methods to deform Ts to Td: the first is a positive deformation, it is coordinate transformation for each point in the source image, get its position in the target image, and then copy the color value; The second is reverse deformation, it is calculated for each point in the target image, get its position in the source image, and then copy the color value. There is a problem with positive deformation, is possible some pixel in the target image has no color values, and reverse deformation can ensure that every point in the target image can find the corresponding point in the original image, so the reverse deformation technology would be used here.

Suppose the vertex of T_s and T_d are respectively corresponded as P_{s1}、P_{s2}、P_{s3} and P_1、P_2、P_3. So, an affine transformation can be uniquely identified by these six points:

$$\begin{bmatrix} P_{sx} \\ P_{sy} \\ 1 \end{bmatrix} = \begin{bmatrix} a_{11} & a_{12} & a_{13} \\ a_{21} & a_{22} & a_{23} \\ 0 & 0 & 1 \end{bmatrix} \begin{bmatrix} P_{dx} \\ P_{dy} \\ 1 \end{bmatrix} \tag{26}$$

P_{dx} and P_{dy} in the formula 26 are x,y coordinate of a point P_d in T_d, P_{xx} and P_{xy} are x,y coordinate of the corresponding point P_y in T_y. Order:

$$A = \begin{bmatrix} a_{11} & a_{12} & a_{13} \\ a_{21} & a_{22} & a_{23} \end{bmatrix} \tag{27}$$

$$A = \begin{bmatrix} P_{S1x} & P_{S2x} & P_{S3x} \\ P_{S1y} & P_{S2y} & P_{S3y} \end{bmatrix} \begin{bmatrix} P_{1x} & P_{2x} & P_{3x} \\ P_{1y} & P_{2y} & P_{3y} \\ 1 & 1 & 1 \end{bmatrix}^{-1} \tag{28}$$

The formula 28 must have a solution as long as the triangle T_d no degradation to a straight line or a point, actually if T_d has degradation, but the boundary of all triangles in the mesh are overlapping with the boundary of the adjacent triangles, the formula insolubility has no influence to the deformation effect of the whole image.

It is important to note that because the triangle movement contains triangle deformation, so the pixels in T_d by affine transformation mapping to T_s are not just in the image pixels within the grid, the (P_{sx},P_{sy}) is not necessarily an integer, then need to get the prediction image by bilinear interpolation.

Suppose the integer part of (P_{sx},P_{sy}) is (P_{sx0},P_{sy0}), So $dx=P_{sx}-P_{dx}$, $dy=P_{sy}-P_{dy}$.

The predict image of T_d defined by the follow formula:

$$\begin{aligned} (P_{dx}, P_{dy}) &= (1-dx)(1-dy)(P_{sx0}, P_{sy0}) + (1-dx)dy(P_{sx0}, P_{sy0}+1) \\ &+ dx(1-dy)(P_{sx0}+1, P_{sy0}) + dxdy(P_{sx0}+1, P_{sy0}+1) \end{aligned} \tag{29}$$

The three-dimensional image of left and right view of the feature points and feature points matching information according to the fourth chapter, then make the left view of Delaunay triangulation subdivision for triangular mesh deformation processing in the fifth chapter, get the reconstruction view of the right, the result is shown in Figure 7.

Figure 7. Result of Morphing

7. Conclusion

A simple method of image deformation process has been used in this article. Although the final reduction stereoscopic image display apparatus having a better stereoscopic effect and clarity, however, in high resolution, the edge of the image still has distinguishable portion of the distortion. Therefore, the search of a higher accuracy deformation algorithm is an important work in the future.

Acknowledgements

This paper is supported by the Programme of Introducing Talents of Discipline to Universities (B13009).

References

[1] A. Abdennour, “An intelligent supervisory system for drum type boilers during severe disturbances”, International Journal of Electrical Power & Energy Systems, vol. 22, no. 5, (**2000**) June, pp. 381-387.
[2] J. Canny, “A Computational Approach to Edge Detection”, IEEE Transactions on Pattern Analysis and M achine Intelligence, vol. 8, no. 6, (**1986**), pp. 679-698.
[3] P. Bao and L. Zhang, “Canny edge detection enhancement by sale Multiplication”, IEEE Trans on Pattern Analysis and Machine Intelligence, (**2005**), vol. 27, no. 9, pp. 1485—1490.
[4] T. and D. J. Heeger, “Perceptual Image Distortion”, In Proc. SPIE Human Vision, Visual Processing and Digital Display, vol. 2179, pp. 127–141, San Jose, CA.
[5] G. Taubin and J. Rossignac, “Geometry compression through topological surgery”, ACM Transactions on Graphics, vol. 17, no. 2, (**1998**), pp. 84-115.
[6] J.-R. Ohm and K. Gruneberg, “A realtime hardware system for 65stereoscopic videoconferencing with viewpoint adaptation”, Signal Processing Image Connunication, (**1998**), pp. 147-171.
[7] A. Certain, J. Popovic, T. DeRose, T. Duchamp, D. Salesin and W. Stuetzle, “Interactive Multiresolution Surface Viewing”, Proc. Of Siggraph 96’, (**1996**), pp. 96-97.
[8] N. P. Weatherill, “Delaunay triangulation in computational fluid dynamics [J]”, Computers Math, Applic., vol.24, (**1992**), pp. 129-150.
[9] G., Taubin, A. Gueziec and W. Horn, “Progressive forest split compression”, Proc, of SIGGRAPH 98’, (**1998**), pp. 123-123.
[10] J.-R. Ohm and K. Gruneberg, “A realtime hardware system for 65stereoscopic videoconferencing with viewpoint adaptation”, Signal Processing Image Connunication, (**1998**), pp. 147-171.

Author

Xiaoyuan Yan
1989.02
Male
Education background: Master's degree
Research direction: The fire image compression and processing